

# Vanadium(IV)–Citrate Complex Interconversions in Aqueous Solutions. A pH-Dependent Synthetic, Structural, Spectroscopic, and Magnetic Study

M. Tsaramyrsi, M. Kaliva, and A. Salifoglou\*

Department of Chemistry, University of Crete, Heraklion 71409, Greece

C. P. Raptopoulou and A. Terzis

Institute of Materials Science, NCSR “Demokritos”, Aghia Paraskevi 15310, Attiki, Greece

V. Tangoulis

Department of Materials Science, University of Patras, Patras 26500, Greece

J. Giapintzakis

Institute of Electronic Structure and Laser, FORTH, Heraklion 71110, Greece

Received March 13, 2001

Citrate is abundantly encountered in biological fluids as a natural metal ion chelator. Vanadium participates in biological processes as a catalyst in the active sites of metalloenzymes, as a metabolic regulator, as a mitogenic activator, and as an insulin-mimicking agent. Thus, vanadium chemistry with natural chelators, such as citrate, may have immediate implications on its role in a cellular milieu, and its action as a biological agent. In an effort to comprehend the aqueous chemistry of one of vanadium's oxidation states, namely, V(IV), implicated in its biological activity, reactions of  $VCl_3$  and citric acid were pursued in water and led to V(IV)–citrate complexes, the nature and properties of which depend strongly on the solution pH. Analytical, FT-IR, UV/vis, EPR, and magnetic susceptibility data supported the formulation of  $X_4\{[VO(H_{-1}Cit)]_2\} \cdot nH_2O$  ( $H_{-1}Cit = C_6H_4O_7^{4-}$ ;  $X = K^+$ ,  $n = 6$  (**1**);  $X = Na^+$ ,  $n = 12$  (**2**);  $X = NH_4^+$ ,  $n = 2$  (**3**)) (pH  $\approx 8$ ) and  $X_3\{[V_2O_2(H_{-1}Cit)(Cit)]\} \cdot nH_2O$  ( $X = K^+$ ,  $n = 7$  (**4**)) (pH  $\approx 5$ ). Complex **2** crystallizes in space group  $P2_1/c$ ,  $a = 11.3335(9)$  Å,  $b = 15.788(1)$  Å,  $c = 8.6960(6)$  Å,  $\beta = 104.874(3)^\circ$ ,  $V = 1503.8(2)$ ,  $Z = 2$ . Complex **3** crystallizes in space group  $P\bar{1}$ ,  $a = 9.405(1)$  Å,  $b = 10.007(1)$  Å,  $c = 13.983(2)$  Å,  $\alpha = 76.358(4)^\circ$ ,  $\beta = 84.056(4)^\circ$ ,  $\gamma = 66.102(4)^\circ$ ,  $V = 1169.2(3)$ ,  $Z = 2$ . Complex **4** crystallizes in space group  $P2_1nb$ ,  $a = 9.679(4)$  Å,  $b = 19.618(8)$  Å,  $c = 28.30(1)$  Å,  $V = 5374.0(4)$ ,  $Z = 8$ . The X-ray structures of **1–4** are  $V_2O_2$  dimers, with the citrate displaying varying coordination numbers and modes. **1** exhibits a small ferromagnetic interaction, whereas **4** exhibits an antiferromagnetic interaction between the V(IV) ions. **1** and **4** interconvert with pH, thus rendering the pH a determining factor promoting variable structural, electronic, and magnetic properties in V(IV)–citrate species. The observed aqueous behavior of **1–4** is consistent with past solution speciation studies, and contributes to the understanding of significant aspects of the biologically relevant vanadium(IV)–citrate chemistry.

## Introduction

The quintessence of citrate in biological processes has been well established.<sup>1</sup> Citrate is a primary metabolite in metabolic cycles (Krebs cycle)<sup>2</sup> and one of the most abundant metal ion binders in cellular fluids (human plasma).<sup>3</sup> Due to the presence

of carboxylate and hydroxo functionalities, citrate extends its chemical reactivity toward a number of bioessential metal ions, among which vanadium stands as a suitable natural target.<sup>2,4</sup> As a metal ion, vanadium occupies active site metalloenzyme centers and is involved in the activation/inhibition of key metabolic enzymes in the biological milieu. Among the metalloenzymes harboring vanadium in their active sites are nitrogenases<sup>5</sup> and haloperoxidases.<sup>6</sup> Prominent among the biological regulatory roles of vanadium stand its mitogenic action<sup>7</sup> and insulin-mimetic activity in humans.<sup>8</sup> A number of

\* To whom correspondence should be addressed. Phone: +30-81-393-652. Fax: +30-81-393-601. E-mail: salif@chemistry.uoc.gr.

- (1) (a) Etcheverry, S. B.; Apella, M. C.; Baran, E. J. *J. Inorg. Biochem.* **1984**, *20*, 269–274. (b) Glusker, J. P. *Acc. Chem. Res.* **1980**, *13*, 345–352.  
 (2) (a) Beinert, H. *FASEB J.* **1990**, *4*, 2483–2491. (b) Lippard, S. J.; Berg, J. M. *Principles of Bioinorganic Chemistry*; University Science Books: Mill Valley, CA, 1994; Chapter 12, pp 352–354.  
 (3) (a) Crans, D. C. In *Metal Ions in Biological Systems: Vanadium and its Role in Life*; Sigel, H., Sigel, A., Eds.; Marcel Dekker: New York, 1995; Chapter 5, pp 147–209. (b) Martin, R. B. *J. Inorg. Biochem.* **1986**, *28*, 181–187.

(4) Rehder, D. *Biomaterials* **1992**, *5*, 3–12.

(5) Liang, J.; Madden, M.; Shah, V. K.; Burrell, R. H. *Biochemistry* **1990**, *29*, 8577–8581.

(6) (a) Vilter, H. In *Metal Ions in Biological Systems: Vanadium and its Role in Life*; Sigel, H., Sigel, A., Eds.; Marcel Dekker: New York, NY, 1995; Chapter 10, pp 325–362. (b) Butler, A.; Walker, J. V. *Chem. Rev.* **1993**, *93*, 1937–1944.

solution studies have been carried out on vanadium(IV,V)–ligand systems in the past, aiming to delineate the biodistribution of species involved in biologically related processes. Concurrently, synthetic studies have targeted biomimetic complexes at both V(V) and V(IV) oxidation states, which have been implicated in enzymic regulation.<sup>7–9</sup> Despite the fact, though, that synthetically isolated V(IV,V) complexes with various ligands are known,<sup>10</sup> detailed investigations into the possible interrelationships among vanadium(IV,V)–citrate synthetic complexes, through the study of their systematic pH-dependent synthesis and exploration of their chemical properties in solution and the solid state, were limited. Such studies could be helpful in (a) establishing the existence of species in biodistribution patterns of vanadium in the presence of specific ligands and (b) unraveling the factor(s) that might be involved in interlinking those species throughout the physiological pH range. Having chosen citrate as the biologically relevant ligand capable of promoting interactions with vanadium ions in solution, we pursued studies targeting structurally characterized, chemically distinct aqueous V(IV)–citrate complexes under conditions prevalent in biological media. Herein, we report on (a) the expedient pH-dependent synthesis and structural, spectroscopic, magnetic, and solution properties of dinuclear anionic V(IV)–citrate complexes, (b) the transformations between two of those V(IV)–citrate complexes in aqueous solution as a function of pH, and (c) the potential implications of their solution chemical structures and properties in biologically relevant solutions.

## Experimental Section

**Materials.** Reagent-grade  $\text{VCl}_3$  and  $\text{C}_6\text{H}_8\text{O}_7$  (Aldrich), KOH and NaOH (Merck),  $\text{NH}_3$  (Riedel-De Haën), and 2-propanol (Fluka) were used. All reactions were carried out in the air. Nanopure-quality water was used throughout this work.

**Physical Measurements.** Elemental analyses were carried out by Quantitative Technologies, Inc. FT-IR spectra were recorded on a Perkin-Elmer 1760X FT-infrared spectrometer, in KBr pellets. UV/vis measurements were taken on a Hitachi U-2001 spectrophotometer, in aqueous solutions. Variable-temperature, solid-state magnetic susceptibility data were collected on powdered samples of complexes **1** and **4**, in a 6.0 kG applied magnetic field and in the temperature ranges 2.0–286 and 6.0–300 K, respectively. Magnetization measurements were carried out at various temperatures from 1.9 to 5 K and in the field range 0–5 T. The solid-state and solution EPR spectra of **1** and **4** were recorded on a Bruker ER 200D-SRC X-band spectrometer, equipped with an Oxford ESR 9 cryostat at 9.174 GHz, 10 dB, and 4 K.

**Preparations.**  $\text{K}_4[\text{V}_2\text{O}_2(\text{C}_6\text{H}_4\text{O}_7)_2]\cdot 6\text{H}_2\text{O}$  (**1**) (MW = 774.58). A 0.09 g sample of  $\text{VCl}_3$  (0.58 mmol) and 0.11 g of citric acid (anhydrous) (0.58 mmol) were mixed in water (5 mL). The pH of the reaction mixture was adjusted to ~8 with an aqueous solution of 0.4 M KOH,

and stirring continued overnight. On the following day, the blue solution was taken to dryness. The residue was redissolved in 2 mL of nanopure  $\text{H}_2\text{O}$ , and 2-propanol was added. Within 2 days, blue crystals formed at 4 °C, which were isolated by filtration and dried in vacuo. The yield was 0.20 g (~89%). Anal. Calcd for  $\text{K}_4\text{V}_2\text{C}_{12}\text{H}_{20}\text{O}_{22}$ : C, 18.60; H, 2.58; K, 20.14. Found: C, 18.67; H, 2.53; K, 19.90.

In a similar reaction, 0.16 g of  $\text{VOSO}_4$  (1.04 mmol) and 0.20 g of citric acid (1.04 mmol) reacted in water (5 mL), and at pH  $\approx$  8 led, upon addition of 2-propanol, to the isolation of large blue crystals. The yield of the reaction was ~50%. FT-infrared spectroscopy and X-ray unit cell determination provided positive identification of the crystalline product as  $\text{K}_4[\text{V}_2\text{O}_2(\text{C}_6\text{H}_4\text{O}_7)_2]\cdot 6\text{H}_2\text{O}$ .

$\text{Na}_4[\text{V}_2\text{O}_2(\text{C}_6\text{H}_4\text{O}_7)_2]\cdot 12\text{H}_2\text{O}$  (**2**) (MW = 818.22). A 0.09 g sample of  $\text{VCl}_3$  (0.58 mmol) and 0.11 g of citric acid (anhydrous) (0.58 mmol) were mixed in water (5 mL). The pH of the reaction mixture was adjusted to ~8 with an aqueous solution of 0.4 M NaOH, and stirring continued overnight. On the following day, the blue solution was taken to dryness. The residue was redissolved in 2 mL of nanopure  $\text{H}_2\text{O}$ , and precipitation with 2-propanol at 4 °C led to a blue crystalline material, which was isolated by filtration and dried in vacuo. The yield was 0.18 g (~77%). Anal. Calcd for  $\text{Na}_4\text{V}_2\text{C}_{12}\text{H}_{20}\text{O}_{28}$ : C, 17.61; H, 3.91; Na, 11.24. Found: C, 17.48; H, 3.82; Na, 11.20.

$(\text{NH}_4)_4[\text{V}_2\text{O}_2(\text{C}_6\text{H}_4\text{O}_7)_2]\cdot 2\text{H}_2\text{O}$  (**3**) (MW = 618.26). A 0.09 g sample of  $\text{VCl}_3$  (0.58 mmol) and 0.11 g of citric acid (anhydrous) (0.58 mmol) were mixed in water (5 mL). The pH of the reaction mixture was adjusted to ~8 with a 1 M aqueous solution of ammonia, and stirring continued overnight. On the following day, the blue solution was taken to dryness. The residue was redissolved in a minimum amount of warm nanopure  $\text{H}_2\text{O}$ . The flask was placed in the refrigerator, and a few days later large blue crystals appeared, which were isolated by filtration and dried in vacuo. The yield was 0.06 g (~34%). Anal. Calcd for  $\text{N}_4\text{V}_2\text{C}_{12}\text{H}_{28}\text{O}_{18}$ : C, 23.31; H, 4.53; N, 9.06. Found: C, 22.79; H, 4.45; N, 9.13.

$\text{K}_3[\text{V}_2\text{O}_2(\text{C}_6\text{H}_4\text{O}_7)(\text{C}_6\text{H}_5\text{O}_7)]\cdot 7\text{H}_2\text{O}$  (**4**) (MW = 754.51). A 0.09 g sample of  $\text{VCl}_3$  (0.58 mmol) and 0.11 g of citric acid (anhydrous) (0.58 mmol) were mixed in water (5 mL). The pH of the reaction mixture was adjusted to ~5 with an aqueous solution of 0.4 M KOH, and stirring continued overnight. On the following day, the blue-green solution was taken to dryness. The residue was redissolved in 2 mL of nanopure  $\text{H}_2\text{O}$ , and 2-propanol was added. The reaction mixture was taken to 4 °C, and blue needlelike crystals were obtained upon standing. The crystals were isolated by filtration and dried in vacuo. The yield was 0.08 g (~36%). Anal. Calcd for  $\text{K}_3\text{V}_2\text{C}_{12}\text{H}_{23}\text{O}_{23}$ : C, 19.10; H, 3.05; K, 15.50. Found: C, 18.99; H, 2.94; K, 15.28.

**Interconversions.** **Conversion of  $\text{K}_3[\text{V}_2\text{O}_2(\text{C}_6\text{H}_4\text{O}_7)(\text{C}_6\text{H}_5\text{O}_7)]\cdot 7\text{H}_2\text{O}$  to  $\text{K}_4[\text{V}_2\text{O}_2(\text{C}_6\text{H}_4\text{O}_7)_2]\cdot 6\text{H}_2\text{O}$ .** A 0.035 g sample of  $\text{K}_3[\text{V}_2\text{O}_2(\text{C}_6\text{H}_4\text{O}_7)(\text{C}_6\text{H}_5\text{O}_7)]\cdot 7\text{H}_2\text{O}$  (0.046 mmol) was placed in an aqueous solution (5 mL). The pH of the resulting solution was adjusted to ~8 with an aqueous solution of 0.4 M KOH, and stirring continued. The blue solution turned pale brown, then blue-gray, and finally after  $\frac{1}{2}$  h of additional stirring permanently blue. The solution was then taken to dryness. The residue was redissolved in 2 mL of nanopure  $\text{H}_2\text{O}$ , and 2-propanol was added. The reaction mixture was stored in the refrigerator for 3 days. Upon standing, a blue crystalline material was obtained which was isolated by filtration and dried in vacuo. The yield was 0.02 g. Positive identification of the crystalline product as  $\text{K}_4[\text{V}_2\text{O}_2(\text{C}_6\text{H}_4\text{O}_7)_2]\cdot 6\text{H}_2\text{O}$  (**1**) was provided by the FT-IR spectrum of the material and X-ray unit cell determination for one of the single crystals obtained.

**Conversion of  $\text{K}_4[\text{V}_2\text{O}_2(\text{C}_6\text{H}_4\text{O}_7)_2]\cdot 6\text{H}_2\text{O}$  to  $\text{K}_3[\text{V}_2\text{O}_2(\text{C}_6\text{H}_4\text{O}_7)(\text{C}_6\text{H}_5\text{O}_7)]\cdot 7\text{H}_2\text{O}$ .** A 0.05 g sample of  $\text{K}_4[\text{V}_2\text{O}_2(\text{C}_6\text{H}_4\text{O}_7)_2]\cdot 6\text{H}_2\text{O}$  (0.065 mmol) was placed in an aqueous solution (1.5 mL). The pH of the resulting solution was adjusted to ~5 with aqueous hydrochloric acid. The reaction solution was stirred overnight, without any change in its blue color. On the following day, 2-propanol was added to the reaction solution, which was subsequently taken to 4 °C. A few days later, blue needlelike crystals appeared at the bottom of the flask, and they were isolated by filtration and dried in vacuo. The yield was 0.02 g. Positive identification of the crystalline product as  $\text{K}_3[\text{V}_2\text{O}_2(\text{C}_6\text{H}_4\text{O}_7)(\text{C}_6\text{H}_5\text{O}_7)]\cdot 7\text{H}_2\text{O}$  (**4**) was provided by the FT-IR spectrum of the material and X-ray unit cell determination for one of the single crystals obtained.

- (7) (a) Stankiewicz, P. J.; Tracey, A. S. In *Metal Ions in Biological Systems: Vanadium and its Role in Life*; Sigel, H., Sigel, A., Eds.; Marcel Dekker: New York, 1995; Chapter 8, pp 265–266. (b) Owada, M. K.; Iwamoto, M.; Koike, T.; Kato, Y. *J. Cell Physiol.* **1989**, *138*, 484–492.
- (8) Orvig, C.; Thompson, K. H.; Batell, M.; McNeill J. H. In *Metal Ions in Biological Systems: Vanadium and its Role in Life*; Sigel, H., Sigel, A., Eds.; Marcel Dekker: New York, 1995; Chapter 17, pp 575–594.
- (9) (a) Percival M. D.; Doherty, K.; Gresser, M. J. *Biochemistry* **1990**, *29*, 2764–2769. (b) Crans, D. C.; Bunch, R. L.; Theisen, L. A. *J. Am. Chem. Soc.* **1989**, *111*, 7597–7607.
- (10) (a) Mahroof-Tahir, M.; Keramidis, A. D.; Goldfarb, R. B.; Anderson, O. P.; Miller, M. M.; Crans, D. C. *Inorg. Chem.* **1997**, *36*, 1657–1668. (b) Wright, D. W.; Humiston, P. A.; Orme-Johnson, W. H.; Davis, W. M. *Inorg. Chem.* **1995**, *34*, 4194–4197. (c) Schulz, D.; Weyhermüller, T.; Wieghardt, K.; Nuber, B. *Inorg. Chim. Acta* **1995**, *240*, 217–229. (d) Fisher, D. C.; Barclay-Peet, S. J.; Balfe, C. A.; Raymond, K. N. *Inorg. Chem.* **1989**, *28*, 4399–4406. (e) Djordjevic, C.; Lee, M.; Sinn, E. *Inorg. Chem.* **1989**, *28*, 719–723.

**Table 1.** Summary of Crystal, Intensity Collection, and Refinement Data for the Compounds  $\text{Na}_4[\text{VO}(\text{C}_6\text{H}_4\text{O}_7)]_2 \cdot 12\text{H}_2\text{O}$  (**2**),  $(\text{NH}_4)_4[\text{VO}(\text{C}_6\text{H}_4\text{O}_7)]_2 \cdot 2\text{H}_2\text{O}$  (**3**), and  $\text{K}_3[\text{V}_2\text{O}_2(\text{C}_6\text{H}_4\text{O}_7)(\text{C}_6\text{H}_5\text{O}_7)] \cdot 7\text{H}_2\text{O}$  (**4**)

	<b>2</b>	<b>3</b>	<b>4</b>
empirical formula	$\text{Na}_4\text{C}_{12}\text{H}_{32}\text{O}_{28}\text{V}_2$	$\text{C}_{12}\text{H}_{28}\text{N}_4\text{O}_{18}\text{V}_2$	$\text{C}_{12}\text{H}_{23}\text{K}_3\text{O}_{23}\text{V}_2$
fw	818.22	618.26	754.51
temp (°C)	25	25	25
wavelength, $\lambda$ (Å)	(Cu K $\alpha$ ) 1.54180	(Cu K $\alpha$ ) 1.54180	(Mo K $\alpha$ ) 0.71073
space group	$P2_1/c$	$P1$	$P2_1/nb$
$a$ (Å)	11.3335(9)	9.405(1)	9.679(4)
$b$ (Å)	15.788(1)	10.007(1)	19.618(8)
$c$ (Å)	8.6960(6)	13.983(2)	28.30(1)
$\alpha$ (deg)		76.358(4)	
$\beta$ (deg)	104.874(3)	84.056(4)	
$\gamma$ (deg)		66.102(4)	
$V$ (Å <sup>3</sup> )	1503.8(2)	1169.2(3)	5374(4)
$Z$	2	2	8
$\rho_{\text{calcd}}/\rho_{\text{obsd}}$ (g/cm <sup>3</sup> )	1.807/1.79	1.756/1.74	1.865/1.83
abs coeff, $\mu$ (cm <sup>-1</sup> )	6.805	7.571	12.58
$R^a$	0.0504	0.0312	0.0486
$R_w^a$	0.1372 <sup>b</sup>	0.0824 <sup>c</sup>	0.1128 <sup>d</sup>

<sup>a</sup>  $R$  values are based on  $F$  values, and  $R_w$  values are based on  $F^2$ ;  $R = \sum ||F_o| - |F_c|| / \sum (|F_o|)$ , and  $R_w = [\sum (w(F_o^2 - F_c^2)^2) / \sum (w(F_o^2)^2)]^{1/2}$ . <sup>b</sup> For 2372 reflections with  $I > 2\sigma(I)$ . <sup>c</sup> For 3607 reflections with  $I > 2\sigma(I)$ . <sup>d</sup> For 5775 reflections with  $I > 2\sigma(I)$ .

**X-ray Crystal Structure Determination.** X-ray-quality crystals of **1–4** were grown from water/2-propanol mixtures. Blocklike blue crystals for **1** (0.10 × 0.20 × 0.20 mm), **2** (0.10 × 0.20 × 0.20 mm), and **3** (0.10 × 0.20 × 0.20 mm) and needlelike crystals for **4** (0.08 × 0.12 × 0.40 mm) were mounted onto glass fibers. Unit cell determination of **1** confirmed the identity of the compound as  $\text{K}_4[\text{V}_2\text{O}_2(\text{C}_6\text{H}_4\text{O}_7)_2] \cdot 6\text{H}_2\text{O}$ , in line with literature data.<sup>11</sup> Single-crystal X-ray diffraction data for **2** and **3** were collected at room temperature on a Nicolet P2<sub>1</sub> four-circle diffractometer, using Cu K $\alpha$  radiation ( $\lambda = 0.15418$  Å) and  $\theta$ - $2\theta$  scans. Intensity data for **4** were collected on a Crystal Logic dual-goniometer diffractometer, using Mo K $\alpha$  radiation ( $\lambda = 0.71073$  Å) and  $\theta$ - $2\theta$  scans. The unit cell dimensions for all crystals were determined by a least-squares fit of 24 reflections in the range  $24^\circ < 2\theta < 54^\circ$  for **1–3** and  $11^\circ < 2\theta < 23^\circ$  for **4**. Three standard reflections were monitored every 97 reflections over the course of data collection for all crystals, and showed less than 3% variation and no decay. Lorentz, polarization, and  $\psi$ -scan absorption corrections were applied using Crystal Logic software. Further crystallographic details: for **2**,  $2\theta_{\text{max}} = 130^\circ$ ; scan speed 3.0 deg/min; scan range  $2.3 + \alpha_1\alpha_2$  separation; number of reflections collected/unique/used, 3830/3724 [ $R_{\text{int}} = 0.0106$ ]/3724; 433 parameters refined;  $[\Delta/\sigma]_{\text{max}} = 0.009$ ;  $[\Delta\rho]_{\text{max}}/[\Delta\rho]_{\text{min}} = 0.723/-0.483$  e/Å<sup>3</sup>;  $R1/wR2$  (for all data), 0.0434/0.1056; for **3**,  $2\theta_{\text{max}} = 130^\circ$ ; scan speed 3.0 deg/min; scan range  $2.5 + \alpha_1\alpha_2$  separation; number of reflections collected/unique/used, 6809/3767 [ $R_{\text{int}} = 0.0124$ ]/3767; 433 parameters refined;  $[\Delta/\sigma]_{\text{max}} = 0.011$ ;  $[\Delta\rho]_{\text{max}}/[\Delta\rho]_{\text{min}} = 0.703/-0.315$  e/Å<sup>3</sup>;  $R1/wR2$  (for all data), 0.0277/0.0661; for **4**,  $2\theta_{\text{max}} = 45^\circ$ ; scan speed 1.7 deg/min; scan range  $2.2 + \alpha_1\alpha_2$  separation; number of reflections collected/unique/used, 7042/7042 [ $R_{\text{int}} = 0.0000$ ]/7042; 775 parameters refined;  $[\Delta/\sigma]_{\text{max}} = 0.014$ ;  $[\Delta\rho]_{\text{max}}/[\Delta\rho]_{\text{min}} = 0.515/-0.408$  e/Å<sup>3</sup>;  $R1/wR2$  (for all data), 0.0684/0.1304.

The structures of **2–4** were solved by direct methods using SHELXS-86,<sup>12</sup> and refined by full-matrix least-squares techniques on  $F^2$  by using SHELXL93.<sup>12</sup> All non-H atoms were refined anisotropically. Hydrogen atoms in **2** and **3** and those of the citrates in **4** were located by difference maps and refined isotropically. No H atoms for the water solvate molecules in **4** were included in the refinement. A summary of crystallographic data is given in Table 1. Selected bond

**Table 2.** Bond Lengths (Å) and Angles (deg) for  $\text{Na}_4[\text{VO}(\text{C}_6\text{H}_4\text{O}_7)]_2 \cdot 12\text{H}_2\text{O}$  (**2**)

V(1)–O(1)	2.030(2)	V(1)–O(5)	2.039(2)
V(1)–O(3)	1.986(2)	V(1)–O(7)	2.003(2)
V(1)–O(3) <sup>a</sup>	2.230(2)	V(1)–O(8)	1.611(2)
O(8)–V(1)–O(3)	105.28(10)	O(7) <sup>a</sup> –V(1)–O(5) <sup>a</sup>	92.01(9)
O(8)–V(1)–O(7) <sup>a</sup>	101.62(11)	O(1)–V(1)–O(5) <sup>a</sup>	178.45(8)
O(3)–V(1)–O(7) <sup>a</sup>	153.03(9)	O(8)–V(1)–O(3) <sup>a</sup>	161.48(10)
O(8)–V(1)–O(1)	94.75(10)	O(3)–V(1)–O(3) <sup>a</sup>	75.27(8)
O(3)–V(1)–O(1)	87.88(8)	O(7) <sup>a</sup> –V(1)–O(3) <sup>a</sup>	79.87(8)
O(7)–V(1)–O(1)	87.99(9)	O(1)–V(1)–O(3) <sup>a</sup>	103.76(8)
O(8)–V(1)–O(5) <sup>a</sup>	86.77(10)	O(5) <sup>a</sup> –V(1)–O(3) <sup>a</sup>	74.71(7)
O(3)–V(1)–O(5) <sup>a</sup>	91.42(8)		

<sup>a</sup> Symmetry transformations used to generate equivalent atoms:  $-x + 2, -y + 2, -z$ .

**Table 3.** Bond Lengths (Å) and Angles (deg) for  $(\text{NH}_4)_4[\text{VO}(\text{C}_6\text{H}_4\text{O}_7)]_2 \cdot 2\text{H}_2\text{O}$  (**3**)

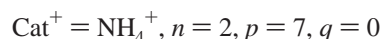
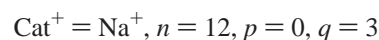
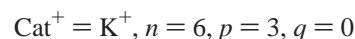
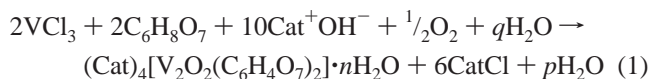
molecule 1		molecule 2	
V(1)–O(1)	2.029(2)	V(2)–O(11)	2.018(2)
V(1)–O(3)	1.964(2)	V(2)–O(13)	1.956(2)
V(1)–O(3) <sup>a</sup>	2.194(2)	V(2)–O(13) <sup>b</sup>	2.192(2)
V(1)–O(5)	2.043(2)	V(2)–O(15)	2.055(2)
V(1)–O(7)	2.018(2)	V(2)–O(17)	2.052(2)
V(1)–O(8)	1.611(2)	V(2)–O(18)	1.608(2)
O(8)–V(1)–O(3)	105.30(8)	O(18)–V(2)–O(13)	107.43(8)
O(8)–V(1)–O(7)	100.78(8)	O(18)–V(2)–O(17)	101.03(8)
O(3)–V(1)–O(7)	153.78(7)	O(13)–V(2)–O(17)	151.43(7)
O(8)–V(1)–O(1)	94.90(8)	O(18)–V(2)–O(11)	96.81(9)
O(3)–V(1)–O(1)	87.84(6)	O(13)–V(2)–O(11)	87.57(6)
O(7)–V(1)–O(1)	87.27(7)	O(11)–V(2)–O(17)	86.64(7)
O(8)–V(1)–O(5)	87.68(8)	O(18)–V(2)–O(15)	89.64(8)
O(3)–V(1)–O(5)	93.21(7)	O(13)–V(2)–O(15)	92.82(7)
O(7)–V(1)–O(5)	90.49(7)	O(17)–V(2)–O(15)	89.76(7)
O(1)–V(1)–O(5)	176.86(6)	O(11)–V(2)–O(15)	173.11(7)
O(8)–V(1)–O(3) <sup>a</sup>	163.78(8)	O(18)–V(2)–O(13) <sup>b</sup>	164.52(8)
O(3)–V(1)–O(3) <sup>a</sup>	75.86(6)	O(13)–V(2)–O(13) <sup>b</sup>	74.68(6)
O(7)–V(1)–O(3) <sup>a</sup>	79.88(6)	O(17)–V(2)–O(13) <sup>b</sup>	78.58(6)
O(1)–V(1)–O(3) <sup>a</sup>	101.32(6)	O(11)–V(2)–O(13) <sup>b</sup>	98.60(6)
O(5)–V(1)–O(3) <sup>a</sup>	76.10(6)	O(15)–V(2)–O(13) <sup>b</sup>	74.90(6)

<sup>a</sup> Symmetry transformations used to generate equivalent atoms:  $-x + 1, -y, -z$ . <sup>b</sup> Symmetry transformations used to generate equivalent atoms:  $-x, -y + 1, -z + 1$ .

length and angle data for all structures determined are given in Tables 2–4.

## Results

**Syntheses.** The syntheses of all complexes reported here were expediently carried out in water, and were based on simple starting materials. Specifically, reactions between  $\text{VCl}_3$  and citric acid in aqueous solutions at  $\text{pH} \approx 8$  led to the isolation of blue crystalline material, upon 2-propanol precipitation (eq 1).



The presence of a base in the reaction mixture was essential, because it not only provided the necessary counterion ( $\text{K}^+$ ,  $\text{Na}^+$ ,  $\text{NH}_4^+$ ) for balancing the charge on the derived anionic complex, but also aided in the adjustment of the pH of the reaction mixture. All of the compounds described here were insoluble

(11) Velayutham, M.; Varghese B.; Subramanian, S. *Inorg. Chem.* **1998**, *37*, 1336–1340.

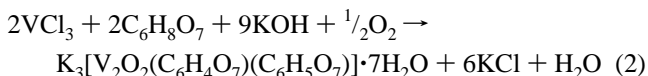
(12) (a) Sheldrick, G. M. *SHELXS-86: Structure Solving Program*; University of Göttingen: Göttingen, Germany, 1986. (b) Sheldrick, G. M. *SHELXL93: Structure Refinement Program*; University of Göttingen: Göttingen, Germany, 1993.

**Table 4.** Bond Lengths (Å) and Angles (deg) for  $K_3[V_2O_2(C_6H_4O_7)(C_6H_5O_7)] \cdot 7H_2O$  (**4**)

molecule 1		molecule 2	
V(1)–O(8)	1.600(6)	V(3)–O(28)	1.593(6)
V(1)–O(1)	1.957(6)	V(3)–O(21)	1.967(6)
V(1)–O(3)	1.992(5)	V(3)–O(23)	1.986(6)
V(1)–O(13)	1.946(5)	V(3)–O(33)	1.958(5)
V(1)–O(15)	1.981(6)	V(3)–O(35)	1.988(6)
V(2)–O(5)	2.426(7)	V(4)–O(25)	2.485(5)
V(2)–O(7)	1.997(7)	V(4)–O(27)	1.987(7)
V(2)–O(11)	1.985(6)	V(4)–O(31)	1.977(6)
V(2)–O(13)	1.974(5)	V(4)–O(33)	1.977(5)
V(2)–O(18)	1.589(7)	V(4)–O(38)	1.580(7)
V(2)–O(3)	1.990(5)	V(4)–O(23)	2.007(5)
O(8)–V(1)–O(3)	105.8(3)	O(28)–V(3)–O(23)	105.8(3)
O(8)–V(1)–O(13)	113.9(3)	O(28)–V(3)–O(33)	111.5(3)
O(13)–V(1)–O(1)	139.7(3)	O(33)–V(3)–O(21)	143.6(3)
O(8)–V(1)–O(15)	105.6(3)	O(28)–V(3)–O(35)	106.3(3)
O(13)–V(1)–O(15)	79.3(2)	O(33)–V(3)–O(35)	79.5(2)
O(1)–V(1)–O(15)	87.7(3)	O(21)–V(3)–O(35)	86.8(2)
O(13)–V(1)–O(3)	80.2(2)	O(33)–V(3)–O(23)	81.2(2)
O(1)–V(1)–O(3)	91.9(2)	O(21)–V(3)–O(23)	93.0(2)
O(15)–V(1)–O(3)	147.4(2)	O(35)–V(3)–O(23)	146.8(2)
O(8)–V(1)–O(1)	106.3(3)	O(28)–V(3)–O(21)	104.8(3)
O(18)–V(2)–O(13)	101.3(3)	O(38)–V(4)–O(33)	102.4(3)
O(18)–V(2)–O(11)	102.1(3)	O(38)–V(4)–O(31)	101.0(3)
O(13)–V(2)–O(11)	89.2(2)	O(33)–V(4)–O(31)	89.2(2)
O(18)–V(2)–O(3)	104.7(3)	O(38)–V(4)–O(23)	106.0(3)
O(13)–V(2)–O(3)	79.5(2)	O(33)–V(4)–O(23)	80.2(2)
O(11)–V(2)–O(3)	152.5(3)	O(31)–V(4)–O(23)	152.5(3)
O(18)–V(2)–O(7)	98.8(3)	O(38)–V(4)–O(27)	99.0(3)
O(13)–V(2)–O(7)	159.7(3)	O(33)–V(4)–O(27)	158.5(3)
O(11)–V(2)–O(7)	89.4(3)	O(31)–V(4)–O(27)	88.1(3)
O(3)–V(2)–O(7)	92.7(2)	O(23)–V(4)–O(27)	92.6(2)
O(18)–V(2)–O(5)	173.6(3)	O(38)–V(4)–O(25)	173.0(3)
O(13)–V(2)–O(5)	81.8(2)	O(33)–V(4)–O(25)	79.6(3)
O(11)–V(2)–O(5)	83.4(3)	O(31)–V(4)–O(25)	85.6(3)
O(3)–V(2)–O(5)	70.2(2)	O(23)–V(4)–O(25)	67.6(3)
O(7)–V(2)–O(5)	77.9(3)	O(27)–V(4)–O(25)	79.0(3)

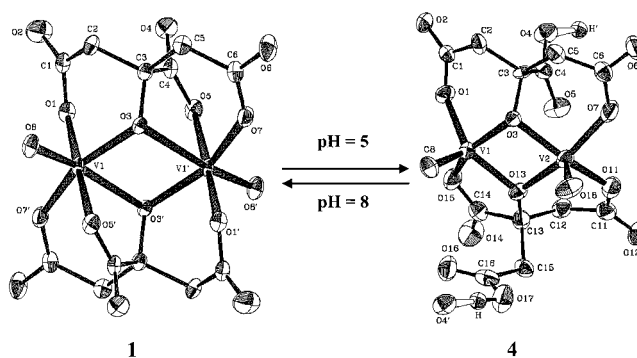
in alcohols and organic solvents, and soluble in water. Elemental analyses on the isolated compounds led to the proposed formulae ( $X_4[\{VO(H_{-1}Cit)\}_2] \cdot nH_2O$  ( $H_{-1}Cit = C_6H_4O_7^{4-}$ ;  $X = K^+$ ,  $n = 6$  (**1**);  $X = Na^+$ ,  $n = 12$  (**2**);  $X = NH_4^+$ ,  $n = 2$  (**3**))). X-ray crystallography was instrumental in further confirming<sup>11</sup> and/or unraveling the identity of the compounds in the solid state (vide infra).

In an effort to investigate the pH dependence of the aforementioned reactions, a representative reaction was run with the same starting materials and metal to citrate stoichiometry (1:1) at pH  $\approx 5$ . Under such fairly acidic conditions, achieved with the help of KOH, addition of 2-propanol led to the precipitation and subsequent isolation of blue needlelike crystals (eq 2). The rationale for choosing these specific conditions to

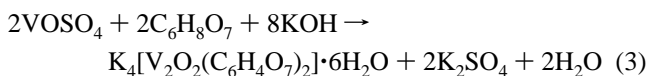


run the reaction was similar to that used in the reactions run at alkaline pH. The isolated blue crystalline material was insoluble in alcohols and organic solvents and soluble in water. Elemental analyses led to the proposed formula ( $X_3[V_2O_2(H_{-1}Cit)(Cit)] \cdot nH_2O$  ( $X = K^+$ ,  $n = 7$  (**4**))). It appears, therefore, that, under the experimental conditions employed, pH is a significant factor in determining the nature of the product of the reaction between  $VCl_3$  and citric acid.

It should be mentioned here that, in both cases of aqueous reactions 1 and 2, run at two different pH values, the isolated end product contained vanadium in the oxidation state +4.

**Figure 1.** Interconversion of complexes **1** and **4**. ORTEP structures of the  $[VO(C_6H_4O_7)]_2^{4-}$  and  $[V_2O_2(C_6H_5O_7)(C_6H_4O_7)]^{3-}$  anions with the atom labeling schemes in **1** and **4**, respectively. Thermal ellipsoids are drawn by ORTEP and represent 50% probability surfaces.

Therefore, under the employed reaction conditions, the initially introduced V(III) was oxidized to V(IV). The fact that oxidation was involved in the synthesis of **1–4** did not affect either the nature of the products themselves or the yields of the respective reactions when V(IV) was used as a starting material. To that end,  $VOSO_4$  reacted equally well with citric acid, and at pH  $\approx 8$  led to the isolation of **1** at comparable yields (eq 3).



**Interconversions.** In an attempt to explore the solution properties of **1** and **4**, it was found that these complexes interconvert by merely adjusting the solution pH to 5 or 8 (Figure 1). Simple dissolution of **4** in water and subsequent adjustment of the pH of the solution to  $\sim 8$  led, upon 2-propanol addition, to the precipitation of blue crystalline material. FT-infrared spectroscopy and X-ray unit cell determination offered positive identification of the pH  $\approx 8$  product as  $K_4[V_2O_2(C_6H_4O_7)_2] \cdot 6H_2O$ . In an analogous fashion, dissolution of **1** in water and subsequent adjustment of the pH to  $\sim 5$  with hydrochloric acid resulted in the isolation of blue crystalline material **4** upon addition of 2-propanol. The FT-infrared spectrum of the material and X-ray unit cell determination of a single crystal provided positive identification of the pH  $\approx 5$  product as  $K_3[V_2O_2(C_6H_4O_7)(C_6H_5O_7)] \cdot 7H_2O$ .

The conversion of **4** to **1** and vice versa, in aqueous solutions, through the mere adjustment of pH offers an alternative route to the synthesis of the two complexes, beyond the self-assembly redox synthetic route of the initially described reactions. Further, this interconversion behavior indicates that pH can promote drastic structural changes in aqueous V(IV)–citrate complex chemistry under the examined reaction conditions.

**Description of the Structures.**  $X_4[\{VO(H_{-1}Cit)\}_2] \cdot nH_2O$  ( $X = K^+$ ,  $n = 6$  (**1**);  $X = Na^+$ ,  $n = 12$  (**2**);  $X = NH_4^+$ ,  $n = 2$  (**3**)). The X-ray crystal structure of **1** was reported before.<sup>11</sup> In the case of complex **2**, the structure reported in the past had a different unit cell from the one reported here.<sup>13</sup> In addition, the number of water molecules in the lattice of **2**, reported in the past, is six compared to twelve found in our crystals.<sup>13</sup> Therefore, the structures of **2** and **3** are reported here together. Complex **3** crystallizes in space group  $P\bar{1}$  with two crystallographically independent molecules per asymmetric unit. In both **2** and **3**, centrosymmetric dinuclear complex anions (Figure 1)  $[\{VO(C_6H_4O_7)\}_2]^{4-}$  are present, with two V=O groups linked

(13) Zhou, Z.-H.; Wan, H.-L.; Hu, S.-Z.; Tsai, K.-R. *Inorg. Chim. Acta* **1995**, *237*, 193–197.

trans to the central hydroxo oxygens of two citrate ligands. The citrates are fully deprotonated and utilize all of their binding sites to coordinate to the two V(IV) ions. Consequently, both V(IV) ions achieve octahedral coordination. All three carboxylate groups on each citrate ligand bind to vanadium as monodentate ligands. Moreover, each citrate ligand spans both V(IV) ions, thus satisfying the coordination requirements of the two metal ions. The resulting  $V^{IV}_2O_2$  rhombic core unit contains two V=O moieties in an anti coplanar configuration. The two V(IV) ions in the distorted octahedra of **2** and **3** exhibit V—O and  $V^{IV}=O$  distances (Figure 1) in the range of those observed in similar dinuclear complexes such as **1**,<sup>11</sup>  $Na_4[V_2O_2\{(O)_2P(O)CH_2N(CH_2COO)_2\}_2] \cdot 10H_2O$  (**5**) (1.985(3)—2.065(3) Å (V—O) and 1.608(4) Å (V=O)),<sup>14</sup>  $[V^{IV}O(Hsabhea)]_2 \cdot 2MeOH$  ( $H_3sabhea = N$ -salicylidene-2-(bis(2-hydroxyethyl)amino)ethylamine) (**6**) (1.938(2)—2.079(2) Å (V—O) and 1.626(2) Å (V=O)),<sup>15</sup>  $(NH_4)_4[V_2O_2(OH)(C_4O_4)_2(H_2O)_3] \cdot H_2O$  (**7**) (1.922(15)—2.331(21) Å (V—O) and 1.549(23)—1.567(22) Å (V=O)),<sup>16</sup> and  $Na_4\{[V_2O_2(H-Cit)]_2\} \cdot 6H_2O$  (**8**) (1.971(2)—2.206(2) Å (V—O) and 1.610(2) Å (V=O)).<sup>13</sup> The observed anti coplanar (V=O)<sub>2</sub>O<sub>2</sub> configuration in **2** and **3** can only be seen in **6** and **8**. The equatorial angles around each vanadium in the  $V_2O_2$  core in **2** and **3** are in the range of those observed in **5** (74.4(2)—105.9(2)°), **6** (73.03(7)—104.98(9)°), **7** (75.1(8)—104.2(10)°), and **8** (75.05(6)—105.6(8)°). Therefore, the structural data—regardless of the cation used for the crystallization of the 4- anionic complex—point to the stability of the  $V_2O_2$ -core-containing assembly, once the latter forms in solution and is subsequently led to crystallization. The sodium ions in **2** are in contact with water molecules of crystallization as well as with oxygens from the citrates and the oxo group in a distance range of 2.321(3)—2.541(3) Å (six contacts). The presence of water molecules of crystallization as well as citrate oxygens in **2** and **3** is responsible for the extensive hydrogen-bonding network formed in both compounds.

$X_3\{[V_2O_2(H-Cit)(Cit)]\} \cdot nH_2O$  ( $X = K^+$ ,  $n = 7$  (**4**)). Complex **4** crystallizes in space group  $P2_1nb$  with two crystallographically independent molecules per asymmetric unit. The X-ray crystal structure of **4** reveals (Figure 1) a dinuclear complex,  $[V_2O_2(C_6H_5O_7)(C_6H_4O_7)]^{3-}$ , the structural features of which are different from those in **2** and **3**. The scaffold, on which the dinuclear complex is based, consists of a  $V_2O_2$  core. Each vanadium is in the +4 oxidation state and doubly bonded to one oxygen. The two V=O groups are syn to each other, and the two V(IV) ions are deemed square pyramidal. The two citrate ligands utilize different binding sites to coordinate to each vanadium, thus differentiating their coordination modes to the  $V_2O_2$  core. One citrate is coordinated to both vanadyl units through the central hydroxo and the two terminal carboxylate groups, leaving the central carboxylate free. The other citrate coordinates to both vanadyl units through the central hydroxo and carboxylate groups as well as one of the two terminal carboxylates, leaving the second terminal carboxylate group free. The latter carboxylate group is protonated and hydrogen-bonded to the central uncoordinated carboxylate group of an adjacent molecule  $[HO(17) \cdots O(4')]$  ( $1 + x, y, z = 1.433$  Å,  $O(17) \cdots O(4') = 2.589$  Å,  $O(17)-HO(17) \cdots O(4') = 163.2^\circ$ ). In the square pyramidal V(IV) ion of **4**, the V=O (1.580(7)—1.600(6) Å) and V—O (1.946(5)—2.007(5) Å) distances are (Figure 1) similar to those observed in square pyramidal V(IV)-

containing complexes such as  $[V^{IV}O(SALAHE)]_2$  ( $H_2SALAHE = 2$ -(salicylideneamino)-1-hydroxyethane) (**9**) (1.888(10)—1.985(10) Å (V—O) and 1.548(9)—1.619(10) Å (V=O)),<sup>17</sup>  $(Bu_4N)_2[(VO)(Dcp)_2]$  ( $H_3Dcp = 3,5$ -dicarboxypyrazole) (1.981(7)—2.032(8) Å (V—O<sub>av</sub>) and 1.56—1.57 Å ( $V^{IV}=O$ )),<sup>18</sup>  $Na_2\{[(VO)(3-hydroxy-3-methylglutarate)]_2 \cdot MeOH \cdot 3H_2O$  (**10**) (1.953(8)—2.076(23) Å (V—O) and 1.581(8)—1.584(8) Å (V=O)),<sup>19</sup> and  $(NH_4)_2\{[V^{IV}(O)_2]_2[V^{IV}(O)](\mu(-)-quinato(3-))_2\} \cdot H_2O$  (**11**) (1.930(2)—1.959(2) Å (V—O) and 1.611(3) Å ( $V^{IV}=O$ )).<sup>20</sup>

The angles around each vanadium in the  $V_2O_2$  core are in the range of those observed in **9** (77.1(4)—113.2(5)°), **10** (71.5(7)—125.7(53)°), and **11** (75.36(9)—113.1(1)°). With respect to the reported complex  $(Hneo)_2[(VO)_2(cit)(Hcit)] \cdot 4H_2O$  ( $neo = 2,9$ -dimethyl-1,10-phenanthroline) (**12**) (1.948(4)—2.303(5) Å (V—O) and 1.590(5)—1.595(4) Å ( $V^{IV}=O$ )),<sup>21</sup> it should be noted that, despite the general similarities observed in the structures of **4** and **12**, there exist structural differences between the two complexes. These differences pertain both to V—O distances and the O—V—O angles, formed between the V(IV) and the oxygens of the variably coordinated citrate ligands in each complex anion. Such differences may reflect corresponding differences in crystal packing forces, operating in the respective lattices of **4** and **12**. In turn, the different lattices likely arise from the use of the different counterions,  $K^+$  in the case of **4**, and  $Hneo^+$  in the case of **12**, in the crystallization of the two complexes. Notable differences between the two complexes include the following: (a) The V—O distance trans to the V=O bond in the octahedral site of the respective complexes. This V—O distance in **4** is 2.426(7) and 2.485(5) Å (for molecule 1 and molecule 2, respectively), whereas the corresponding distance in **12** is 2.303(5) Å. In view of this difference, the two vanadium sites in **4** were deemed square pyramidal, while in **12**, one of the sites had been deemed square pyramidal, with the second one being octahedral.<sup>21</sup> (b) The V—V distance, which is 3.026(2) and 3.012(2) Å (for molecule 1 and molecule 2, respectively) in **4**, compared to 2.949(2) Å in **12**. (c) The largest angle around the square pyramidal vanadium in **4**, which is 114.0(3)° compared to 109.3(2)° in **12**, thus creating a difference between the two angular values for the same vanadium site in the two complexes. The potassium ions in **4** are in contact with water molecules of crystallization as well as citrate and doubly bonded oxygens at distances in the range 2.706(3)—3.374(3) Å (eight contacts). The water molecules of crystallization, along with the citrate oxygens, are responsible for the extensive hydrogen-bonding network formed.

**UV/Vis Spectroscopy.** The electronic spectra of **1** and **4** were recorded in  $H_2O$  at pH  $\approx$  8 and 5, respectively. The spectrum of **1** showed bands at 217 nm ( $\epsilon = 6000$ ), 262 nm ( $\epsilon = 3600$ ), 320 nm (sh) ( $\epsilon \approx 720$ ), 560 nm ( $\epsilon = 27$ ), and 700 nm (sh) ( $\epsilon \approx 18$ ). The spectrum of **4** showed bands at 213 nm ( $\epsilon = 6100$ ), 303 nm ( $\epsilon = 992$ ), 560 nm ( $\epsilon = 67$ ), and 700 nm (sh) ( $\epsilon \approx 47$ ). In both cases, tentative assignments to d—d transitions could be made for the spectral features above 500 nm. Similar d—d transitions were previously observed for other vanadyl-containing species in the range 500—1000 nm.<sup>22</sup> The features below 350 nm (appearing well into the UV) could be reasonably

(14) Crans, D. C.; Jiang, F.; Anderson, O. P.; Miller, S. M. *Inorg. Chem.* **1998**, *37*, 6645—6655.

(15) Plass, W. *Angew. Chem., Int. Ed. Engl.* **1996**, *35*, 627—631.

(16) Khan, M. I.; Chang, Y.-D.; Chen, Q.; Salta, J.; Lee, Y.-S.; O'Connor, C. J.; Zubieta, J. *Inorg. Chem.* **1994**, *33*, 6340—6350.

(17) Carrano, C. J.; Nunn, C. M.; Quan, R.; Bonadies, J. A.; Pecoraro, V. L. *Inorg. Chem.* **1990**, *29*, 944—951.

(18) Hahn, C. W.; Rasmussen, P. G.; Bayon, J. C. *Inorg. Chem.* **1992**, *31*, 1963—1965.

(19) Castro, S. L.; Cass, M. E.; Hollander, F. J.; Bartley, S. L. *Inorg. Chem.* **1995**, *34*, 466—472.

(20) Codd, A.; Hambley, T. W.; Lay, P. A. *Inorg. Chem.* **1995**, *34*, 877—882.

(21) Burojevic, S.; Shweky, I.; Bino, A.; Summers, D. A.; Thompson, R. C. *Inorg. Chim. Acta* **1996**, *251*, 75—79.

attributed to charge-transfer bands, in line with past observations in the literature.<sup>22</sup>

**FT-IR Spectroscopy.** The FT-infrared spectra of **1–4** showed well-resolved strong and sharp absorption bands for the carboxylate carbonyls of the coordinated citrates. Antisymmetric stretching vibrations  $\nu_{\text{as}}(\text{COO}^-)$  were observed between 1636 and 1600  $\text{cm}^{-1}$ . The corresponding symmetric stretches  $\nu_{\text{s}}(\text{COO}^-)$  appeared between 1425 and 1330  $\text{cm}^{-1}$ . All of the carbonyl absorptions were shifted to lower frequencies with respect to those of free citric acid. The frequency difference  $\Delta(\nu_{\text{as}}(\text{COO}^-) - \nu_{\text{s}}(\text{COO}^-))$ <sup>23</sup> was greater than 200  $\text{cm}^{-1}$ , indicating that carboxylate groups were either free or coordinated to the metal ion in a monodentate fashion. This observation was in agreement with the observed X-ray crystal structures of **1–4**. The aforementioned tentative assignments were, also, in consonance with previous reports on carboxylic acid complexes of various metals.<sup>24</sup> The V=O stretches appeared in the region 935–993  $\text{cm}^{-1}$  for **1–4**. These frequencies were in the range of values observed for other V=O-containing dinuclear species.<sup>14,17,19</sup>

**EPR Spectroscopy.** The X-band powder and solution EPR spectra of **1** at 4 K confirmed the weak ferromagnetic character ( $S = 1$ ) of the intramolecular interaction between the two V(IV) ions. Briefly, the powder EPR spectrum of **1** at 4 K exhibited a signal around  $g = 1.95$  along with a weak signal at  $g = 4.0$ , which corresponds to the half-field transition, revealing the weak ferromagnetic character ( $S = 1$ ) of the interaction between the two V<sup>IV</sup> ions. The presence of the triplet  $S = 1$  state was further supported by the EPR spectrum of **1** in aqueous solution at 4 K. Specifically, the spectrum showed overlapping low- and high-field parallel and perpendicular transitions ( $A_{\perp} = 35$  G,  $A_{\parallel} = 70$  G) ( $> 15$  lines) in the  $\Delta M_s = \pm 1$  region. A weak transition also occurred at  $g \approx 4$ , as a result of the “forbidden”  $\Delta M_s = \pm 2$  triplet–singlet transitions exhibiting hyperfine structure ( $A = 63$  G). The spectral data (see the Supporting Information) were consistent with those previously reported in detail in the literature.<sup>11</sup> The EPR spectrum of **4** at 4 K exhibited a very weak signal at  $g = 2$ , indicating the presence of a paramagnetic impurity.

**Magnetic Susceptibility Studies.** The temperature dependence of  $\chi_{\text{M}}T$  for complex **1** revealed a plateau from room temperature to 50 K, with a value of 0.75  $\text{cm}^3 \text{mol}^{-1} \text{K}$ , which is expected for two uncoupled  $S = 1/2$  spins, and then drastically increased with decreasing temperature to the value of 0.89  $\text{cm}^3 \text{mol}^{-1} \text{K}$  at 2 K. The data were consistent with the presence of a small ferromagnetic ( $S = 1$ ) interaction ( $J = 0.5 \text{ cm}^{-1}$ ,  $g = 1.99$ ) between the two V(IV) ions (Figure 2).<sup>15</sup>

The temperature dependence of  $\chi_{\text{M}}$  for **4** shows that  $\chi_{\text{M}}$  increases drastically from  $17 \times 10^{-4} \text{ cm}^3 \text{mol}^{-1}$  at room temperature to a maximum value of  $24.5 \times 10^{-4} \text{ cm}^3 \text{mol}^{-1}$  at

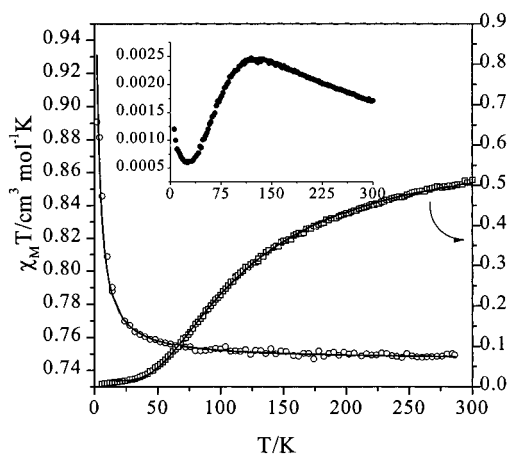


**Figure 2.** Temperature dependence of the magnetic susceptibility of compound **1** (open circles) and compound **4** (open squares), in the form of  $\chi_{\text{M}}T$ , at 6000 G. The solid lines represent the fitting results (see the text). In the inset, the magnetic susceptibility of compound **4** is shown in the form of  $\chi_{\text{M}}$ , at 6000 G.

130 K. Then  $\chi_{\text{M}}$  decreases drastically to a minimum value of  $5 \times 10^{-4} \text{ cm}^3 \text{mol}^{-1}$  at 23 K. From that temperature down to 6 K,  $\chi_{\text{M}}$  increases again to the value of  $12 \times 10^{-4} \text{ cm}^3 \text{mol}^{-1}$  (inset of Figure 2). On the basis of the value of  $\chi_{\text{M}}T$  (0.5  $\text{cm}^3 \text{mol}^{-1} \text{K}$ ), which is smaller than the value expected for two uncoupled spins  $S = 1/2$  for complex **4** at room temperature, and the maximum observed in the temperature dependence of the susceptibility data at 130 K, an antiferromagnetic interaction is expected between the two metal ions. The Curie tail, in the low-temperature susceptibility data, shows the existence of a paramagnetic impurity in the system (possibly a monomer of V(IV)). The overall data are consistent with a strong antiferromagnetic interaction between the two V(IV) ions ( $J = -37.4 \text{ cm}^{-1}$ ,  $g = 1.95(3)$ ), and an  $S = 0$  (Figure 2). Thus, both magnetic susceptibility and EPR data corroborate a clear electronic and magnetic differentiation between **1** and **4**.

The  $\chi_{\text{M}}T$  vs  $T$  for complexes **1** and **4**, and the  $\chi_{\text{M}}$  vs  $T$  for complex **4** data are shown in Figure 2. The data were fitted to the Bleany–Bowers equation (eq 4)<sup>25</sup> based on the zero-field

$$\chi_{\text{M}} = \frac{2Ng^2\mu_{\text{B}}^2}{kT} \frac{1}{3 + \exp(2x)} (1 - \rho) + \frac{\rho Ng^2\mu_{\text{B}}^2}{4kT} \quad (4)$$

spin Hamiltonian  $\hat{H} = -2J\hat{S}_1\hat{S}_2$ , and corrected for the presence of mononuclear impurities, where  $\chi = -J/kT$ ,  $N$  is Avogadro's number,  $\rho$  is the mole fraction of the mononuclear impurity, and the other symbols have the usual meanings. The data were satisfactorily fit into eq 4 with  $J = 0.5 \text{ cm}^{-1}$ ,  $g = 1.99$ , and  $R = 5.4 \times 10^{-6}$  for **1**, and  $J = -37.4 \text{ cm}^{-1}$ ,  $g = 1.95$ ,  $\rho = 0.037$ , and  $R = 3.0 \times 10^{-6}$  for **4**, where  $R$  is the quality of the fit, defined by

$$R = \frac{((\chi T)_{\text{exptl}} - (\chi T)_{\text{calcd}})^2}{(\chi T)_{\text{exptl}}^2}$$

The value of  $g$  for **4** is low, although similar values have been reported in the past.<sup>26</sup> It likely reflects the importance of the hydrogen bonding, which in this case is very strong, revealing a possible 1-D magnetic behavior of the system.

- (22) (a) Ceccato, A. S.; Neves, A.; de Brito, M. A.; Drechsel, S. M.; Mangrich, A. S.; Werner, R.; Haase, W.; Bortoluzzi, A. J. *J. Chem. Soc., Dalton Trans.* **2000**, 1573–1577. (b) Lever, A. B. P. In *Inorganic Electronic Spectroscopy*, 2nd ed.; Elsevier: Amsterdam, 1984; pp 384–392. (c) Robbins, D. J.; Stillman, M. J.; Thomson, A. J. *J. Chem. Soc., Dalton Trans.* **1974**, 813–820. (d) Syamal, A.; Theriot, L. J. *J. Coord. Chem.* **1973**, 2, 193–200. (e) Lee, C. C.; Syamal, A.; Theriot, L. J. *Inorg. Chem.* **1971**, 10, 1669–1673. (f) Sacconi, L.; Campigli, U. *Inorg. Chem.* **1966**, 5, 606–611.
- (23) (a) Djordjevic, C.; Lee, M.; Sinn, E. *Inorg. Chem.* **1989**, 28, 719–723. (b) Deacon, G. B.; Philips, R. J. *Coord. Chem. Rev.* **1980**, 33, 227–250.
- (24) (a) Matzapetakis, M.; Raptopoulou, C. P.; Tsohos, A.; Papefthymiou, B.; Moon, N.; Salifoglou, A. *J. Am. Chem. Soc.* **1998**, 120, 13266–13267. (b) Matzapetakis, M.; Raptopoulou, C. P.; Terzis, A.; Lakatos, A.; Kiss, T.; Salifoglou, A. *Inorg. Chem.* **1999**, 38, 618–619. (c) Tsaramyrsi, M.; Kavousanaki, D.; Raptopoulou, C. P.; Terzis, A.; Salifoglou, A. *Inorg. Chim. Acta* **2001**, 320, 47–59.

- (25) Bleany, B.; Bowers, K. D. *Proc. R. Soc. London, Ser. A* **1952**, 214, 451.
- (26) Rambo, J. R.; Castro, S. L.; Foltling, K.; Bartley, S. L.; Heintz, R. A.; Christou, G. *Inorg. Chem.* **1996**, 35, 6844–6852.

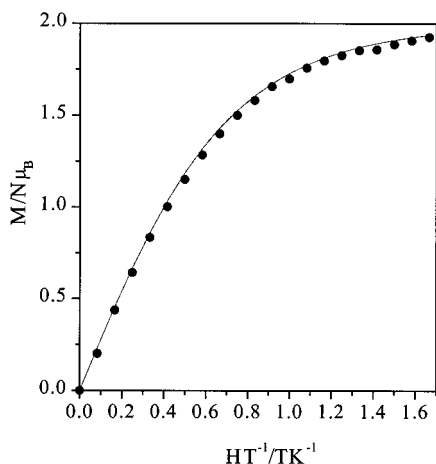


**Figure 3.** Magnetization for compound **1**, in the form of  $M/N\mu_B$ , at 3 K and in the field range 0–5 T. The solid line represents the best fit according to the theoretical Brillouin function for spin  $S = 1$ .

The magnetization measurements are in line with the susceptibility data. For complex **1**, a Brillouin function for an  $S = 1$  system simulated very well the isothermal curve at 3 K (Figure 3), while for complex **4** the existence of a small paramagnetic impurity was reflected in the nonzero magnetization data. These data were simulated by using 3.5% of the Brillouin function of an  $S = 1/2$  system, in accordance with the fitting results.

## Discussion

Simple starting materials, including  $VCl_3$  and citric acid, were employed in the expedient pH-dependent synthesis of dinuclear vanadium complexes **1–4**, containing the  $V_2O_2$  core and two citrate ligands bound to it. In all cases of the synthetic reactions leading to **1–4**, oxidation of V(III) to V(IV) was observed, and pure crystalline materials were obtained. The synthesis of one of the vanadium(IV) complexes, namely, **1**, was also examined and confirmed with the use of  $VOSO_4$  and citric acid. Complexes **1–3** were recovered through the alkaline pH synthetic route, whereas complex **4** was obtained via the low pH synthetic route employed in this study. The X-ray structural investigations of the two pH-dependent classes of complexes proved that the isolated crystalline products contained the rhombic  $V_2O_2$  unit, thus confirming the robustness of that core in all of these compounds, irrespective of the pH used in their syntheses. Given the pH-dependent chemistry, therefore, investigated in the specific reaction system of  $VCl_3$  and citric acid, with a 1:1 molar ratio, it appears that the following features were retained in the structures of both classes of the derived anionic complexes: (a) the  $V_2O_2$  planar rhombic core, (b) the +4 oxidation state of the two vanadium ions comprising the  $V_2O_2$  core, (c) both hydroxo and carboxylate binding sites in the citrate ligands being utilized in their coordination spanning over the two vanadium ions of the  $V_2O_2$  core, and (d) the anionic charge of the complex containing the  $V_2O_2$  core (albeit different for the two classes of complexes **1–3** and **4**).

The structural features that differentiate the two classes of anionic complexes are the following:

(a) The anti coplanar conformation of the  $V=O$  units with respect to the  $V_2O_2$  core in the pH 8 complexes, as opposed to the syn conformation of the  $V=O$  units with respect to the  $V_2O_2$  core in the pH 5 compound. This pH-dependent conformational rearrangement of the two  $V=O$  units, in the two types of complexes, was consistent with the structure of the anionic assemblies emerging from the variable coordination mode of the citrate carboxylates around the  $V_2O_2$  cores.

(b) The protonation state of the two citrate ligands. Specifically, in the structures of the pH 8 complexes, both citrate ligands were fully deprotonated, thus utilizing all of their binding sites to fulfill the coordination requirements of the two octahedral vanadium(IV) ions. In the structure of the pH 5 complex, one of the citrate ligands was fully deprotonated, while the other one was triply deprotonated. Similar protonation state differences in the ligands attached to vanadium were observed in the case of the  $V_2O_2$ -core-containing vanadium(V)-peroxo-malic complexes, which were also synthesized in a pH-dependent manner and isolated from aqueous solutions.<sup>27</sup>

(c) The coordination number of both vanadium ions in the structures of the pH 8 complexes being six (octahedral), while in the pH 5 complex the coordination number was 5 (square pyramidal).

(d) The coordination modes of the two citrate ligands to the vanadium ions in the  $V_2O_2$  core of the pH 5 complex being different. Specifically, the fully deprotonated citrate ligand in **4** employed the two terminal carboxylate groups and the central hydroxo group to span both vanadium ions, leaving the central carboxylate group unbound. In contrast, the triply deprotonated citrate ligand in **4** employed one of its terminal carboxylate groups and both central hydroxo and carboxylate groups to coordinate to the  $V_2O_2$  core, leaving the second terminal carboxylate group free and protonated.

(e) The symmetrical coordination of the citrates around the  $V_2O_2$  in **2** and **3**, as opposed to the nonsymmetrical arrangement of the citrates around the  $V_2O_2$  core in the anionic assembly of **4**.

(f) The reduction in the V---V distance between the structures in **2** and **3**, and the structure in **4**. That reduction was  $\sim 0.3$  Å.

In view of the differences noted between the two basic structures in **2** and **4**, it appears that, in **4**, the existence of the protonated terminal carboxylate group weighs heavily on the structural integrity of the complex. The presence of the proton contributes significantly to the inability of that group, as a binding site, to participate in the coordination sphere of the vanadium(IV) ions of the  $V_2O_2$  core. Furthermore, the same proton promotes the formation of a hydrogen bond with the deprotonated central carboxylate oxygen of an adjacent molecule, thus forcing the protonated carboxylate group further away from the complex assembly. Undoubtedly, this event consolidates the coordination asymmetry introduced in the molecule, and may contribute to the stability of the anionic assembly as a whole. This phenomenon is pronouncedly evident in **4** and **12**, where different counterions were used for the crystallization of the respective anionic complexes.

Moreover, it appears that the vanadium(IV)-citrate anionic assembly in **4** and **12** harbors a structurally flexible  $V_2O_2$  core. This flexibility does not interfere with or compromise the overall stability of the complex anion. In particular, close examination of the structural features in **4** and **12** shows that there exist differences between the respective  $V_2O_2$  cores, at least in the solid state, which are most likely associated with the presence of the cation used for the crystallization of the complex anion. Such differences include variable changes in the V–V distances, the internal  $V_2O_2$  core angles, and distances as well as angles around each vanadium of the  $V_2O_2$  core coordinated to citrate, in **4** and **12**.

Solid-state and solution EPR spectroscopies of complex **1** in water confirmed the weak ferromagnetic coupling between the two vanadium(IV) ions.<sup>11</sup> Further examination of the spectrum

(27) Kaliva, M.; Giannadaki, T.; Raptopoulou, C. P.; Terzis, A.; Tangoulis, V.; Salifoglou, A. *Inorg. Chem.* **2001**, *40*, 3711–3718.

in solution revealed the close similarities of this spectrum with those recorded in earlier studies reported on vanadium(IV)–citrate systems.<sup>28</sup> In those solution studies, it had been proposed that the observed EPR spectrum for the vanadium(IV)–citrate system represented a dinuclear  $V_2O_2$  species in solution. Therefore, both solid-state and solution studies in the present work were consistent with the existence of a dinuclear ( $V=O$ )<sub>2</sub>O<sub>2</sub> species in solution, for which the structure of the complex is now known. This observation was also in line with past solution speciation studies on the vanadium(V)–citrate systems, advocating the presence of dinuclear  $V^V_2O_2$  core complexes in solution.<sup>29</sup> It appears, therefore, that both the  $V^{IV}_2O_2$  and  $V^V_2O_2$  cores can be stable, as that has been shown for various vanadium–ligand systems in the past,<sup>10,27</sup> and the vanadium(IV)–citrate system studied here under the specified experimental conditions.

The magnetic susceptibility studies of **1** and **4** showed that the two complexes are magnetically distinct, with **1** displaying a weak ferromagnetic coupling ( $S = 1$ ) between the two d<sup>1</sup>-metal ions. This magnetic behavior was further corroborated by magnetization measurements. In line with the magnetic susceptibility results was the X-band solid-state and solution EPR spectroscopies, which provided firm evidence on the existence of the weak ferromagnetic interaction ( $S = 1$ ) between the vanadium(IV) ions in the dinuclear complex **1**. Detailed EPR data on this dimer had been previously reported in the literature.<sup>11</sup> In stark contrast to the aforementioned behavior, complex **4** showed that the two vanadium(IV) ions are antiferromagnetically coupled. Further, comparison of the magnetic behavior of **4** with the magnetic behavior of the known complex **12** showed that the antiferromagnetic coupling constant for **4** was  $J = -37 \text{ cm}^{-1}$  compared to  $J = -192 \text{ cm}^{-1}$  observed in **12**. The weaker antiferromagnetic coupling in **4** is consistent with the larger V–V distance observed in **4** ( $V-V_{av} = 3.019(2) \text{ \AA}$ ) compared to that in **12** ( $2.949(1) \text{ \AA}$ ).<sup>21</sup> Analogous observations were previously noted in a number of antiferromagnetically coupled vanadium(IV) dimers.<sup>19,22a,d,e</sup> Furthermore, the difference in the antiferromagnetic coupling between **4** and **12**, in turn, may be directly related to the different crystal packing constraints imposed upon the  $V_2O_2$  core in **4** and **12**, through the employment of different cations ( $K^+$  in **4** and  $HneO^+$  in **12**) in the isolation and crystallization procedures.

A very significant observation of this study was the ability of the two types of complexes, **1** and **4**, to interconvert upon adjustment of the pH of the solution in which they are placed. The ability to promote interconversion of the two species showed the importance of pH in establishing a linkage between two species in the solution of a system, which contains

vanadium(IV) and citrate. It appears that pH acts efficiently as a molecular switch, and promotes profound molecular changes associated with the two low molecular mass structural components of the present vanadium(IV)–citrate system, under the employed experimental conditions. Consequently, beyond its synthetic utility in the isolation of the two classes of vanadium(IV)–citrate dinuclear complexes, pH can influence the (a) structural, (b) electronic, (c) magnetic, and (d) potential, biologically relevant, chemical properties of the archetype compounds **1** and **4**. It can be envisaged, therefore, that, under biologically relevant conditions and in the specific vanadium–citrate system being examined, species interconversion under the influence of solution pH could be significant, suggesting which types of complexes predominate over others. For this contention to be substantive, however, further speciation studies are needed, detailing the distribution of vanadium(IV)–citrate species, including the dinuclear complexes **1–4** investigated here, all as a function of pH and concentration.

Finally, solution studies in the past have pointed out the importance of oxidation state in the action of vanadium in biological systems.<sup>29,30</sup> In view of the fact that reducing agents (cysteine, glutathione, etc.), present in biological fluids, are capable of reducing V(V) to V(IV), the presence of vanadyl species complexed with abundant natural metal ion chelators, such as citrate, should not be discounted.<sup>31</sup> Thus, vanadyl–citrate complexes may represent key species in the elucidation of the V(IV) role in biological fluids. Recently, a mononuclear vanadyl–maltolate species was evaluated for its insulin-mimetic properties.<sup>8,32</sup> In light of the intricate nature of aqueous vanadium chemistry, the herein reported vanadyl–citrate complexes exemplify logical models for stable, low molecular mass soluble species, likely interlinked in biodistribution patterns of vanadium(IV) in biological media. Continuing pursuit of such structurally and electronically diverse synthetic V(IV) complexes aiming to delineate the role of vanadium in cellular fluids is currently ongoing in our lab.

**Acknowledgment.** This work was supported with funds provided by the Department of Chemistry, University of Crete, Greece. The financial assistance to C.P.R. and A.T. by the Greek Secretariat of Research and Technology is gratefully acknowledged.

**Supporting Information Available:** Tables of X-ray crystal structure refinement data, positional and thermal parameters for **2–4**, and EPR spectroscopic data on complex **1**. This material is available free of charge via the Internet at <http://pubs.acs.org>.

IC010276N

- (28) (a) Kiss, T.; Buglyo, P.; Sanna, D.; Micera, G.; Decock, P.; Dewaele, D. *Inorg. Chim. Acta* **1995**, *239*, 145–153. (b) Dunhill, R. H.; Smith, T. D. *J. Chem. Soc. A* **1968**, 2189–2192.  
(29) Ehde, P. M.; Andersson, I.; Pettersson, L. *Acta Chem. Scand.* **1989**, *43*, 136–143.

- (30) Ehde, P. M.; Andersson, I.; Pettersson, L. *Acta Chem. Scand.* **1986**, *A40*, 489–499.  
(31) Kustin, K.; Robinson, W. E. In *Metal Ions in Biological Systems: Vanadium and its Role in Life*; Sigel, H., Sigel, A., Eds.; Marcel Dekker: New York, 1995; Chapter 15, pp 511–542.  
(32) Yuen, V. G.; Orvig, C.; McNeill, J. H. *Can. J. Physiol. Pharmacol.* **1993**, *71*, 263–269.